Acta Polytechnica CTU Proceedings **18**:10–14, 2018
doi:10.14311/APP.2018.18.0010

available online at http://ojs.cvut.cz/ojs/index.php/app

INSTRUMENTATION OF SPLIT HOPKINSON PRESSURE BAR FOR TESTING OF CELLULAR METALLIC MATERIALS

Jan Falta*, Tomáš Fíla, Petr Zlámal, Marcel Adorna

Czech Technical University in Prague, Faculty of Transportation Sciences, Department of Mechanics and Materials, Konviktská 20, 120 00 Prague 1, Czech Republic

* corresponding author: falta@fd.cvut.cz

Abstract. This paper presents an overview of the custom design instrumentation of a Split Hopkinson Pressure Bar modified for dynamic testing of materials with low mechanical impedance, particularly for cellular metallic materials (e. g. metal foams, laser sintered structures). Design and implementation of the components related to the strain wave measurement based on strain gauges (i.e. strain-gauge measurement unit, power supply unit, filtration) and the components used for the control and synchronization of the experiment, such as module of laser trough-beam photoelectric sensor are summarized in the paper. Aside from the design of the hardware components, the contribution deals also with development of a control software with graphical user interference using LabView (National Instruments, USA) programming environment, that allows selection of parameters of the dynamic tests and their storage for the evaluation of experiments.

Keywords: SHPB, instrumentation, strain-gauge measurement, LabView.

1. Introduction

1.1. Motivation

The mechanical properties of specific metal structures may interest some researchers and engineers because their various behavior at different loading rates. In terms of mechanical behavior, it has been observed that the stress-strain response is closely linked to variation in loading rates. Due to this, it is required to be described material response for loading rates that can be expected after initiation in service [1, 2]. The Split Hopkinson Pressure Bar (SHPB) apparatus has rapidly become the widely used device for material testing at high strain rates [3]. One of the directions in current research using SHPB is the testing of porous structures with regular or irregular internal structure [4–6]. The problem of testing porous materials and investigating the mechanisms of their deformation is dealt with by many authors. A summary of the basic results of these works can be found in the work of G.W. Ma, Z.Q. Ye et al. [7].

1.2. Aims and objectives

The SHPB apparatus located at Department of Mechanics and Materials CTU in Prague, is designed for the research in the field of fast deformation processes of materials and structures with low mechanical impedance. Due to possible change of experimental setup in terms of used measurement bars (currently, both aluminum and PMMA bars are used) and number of strain gauges and their type (foil or semiconductor strain gauges) it was necessary to implement our own design of the components. The main advantages of the proposed instrumentation include full control of the signal processing before it is brought to the digitizing card in the PC. There is no unintentional distortion of the measured signal compared to better, but more complex solved commercially available solutions. The solution is also easily expandable with additional measuring points, implementation of different strain gauge sensors or targeted noise reduction in the selected frequency range. It also implements an ability to synchronize external devices such as high-speed camera operating on the TTL trigger principle. The aim of these partial solutions is to improve quality and reliability of the test components while increasing overall comfort of operation of the SHPB instrumentation.

2. SHPB Setup

The instrumentation was performed on a modified Kolsky SHPB setup. The incident, transmission, and striker bars had the same nominal diameter 20 mm. Material of the bars (usually aluminum alloy EN-AW-7075 or PMMA) varied according to the material tested, but this does not affect the instrumentation. A gas-gun system with 16 bar maximum pressure was used to accelerate the striker bar. The incident bar and the transmission bar had the same length 1600 mm and were supported by eight low-friction polymer-liner slide bearings with aluminum housing. Both the incident and the transmission bars were equipped with the strain gauges for the measurement of deformation waves. The assembly also included a high-speed camera for optical inspection of the experiment. Schematically, the entire assembly is depicted in Figure 1, where the main parts of the instrumentation are three in-house designed hardware units (strain-gauge measurement unit, power supply unit and laser sensor and camera trigger unit)

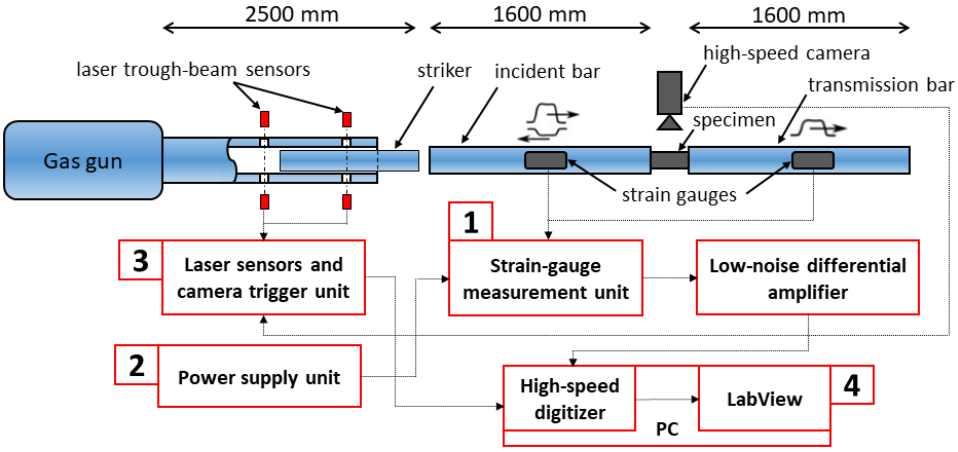

FIGURE 1. SHPB assembly instrumentation scheme.

marked 1-3 and GUI in LabView programing environment marked 4.

3. INSTRUMENTATION

3.1. STRAIN-GAUGE MEASUREMENT UNIT

The basic idea of the solution was the development of a modular assembly of separate measuring cards equipped with resistors matching the type of strain gauge. The simplified circuit diagram for one measuring point is shown in Figure 2. The red framed parts are on the card, the other elements are fixed in the unit. Balancing Wheatstone bridge is implemented using a potentiometer to one of the bridge branches. The measuring cards are located in the sockets with the possibility of replacing by simply pulling out and inserting a different card. An example of a technical solution for placing six cards into the slots within the measuring unit is shown in Figure 3. The module also includes a switch to set bridge configuration to half-bridge or quarter-bridge.

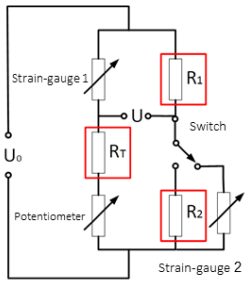

FIGURE 2. Electrical circuit scheme of the realized Wheatstone bridge.

3.2. POWER SUPPLY UNIT

As power supply for strain gauge measurement the custom battery power supply unit was designed. Motivation for the implementation of this unit consisted in the unsatisfactory properties of the laboratory power supplies used so far. The output of the laboratory

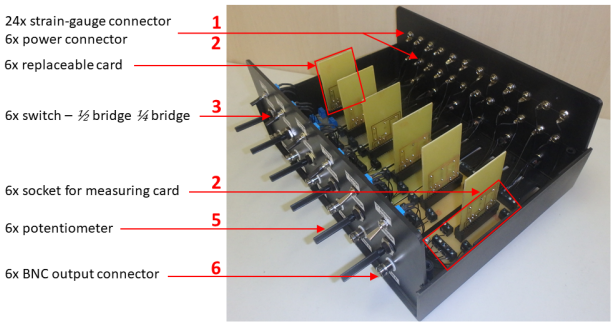

FIGURE 3. Internal distribution of Strain-gauge measurement unit.

power supply exhibited considerable ripple and signal noise and had only a limited number of output terminals. After a series of tests "incident bar apart" void test and "bars together" void test the proper use of the battery sources has been proven to have a less ripple and noise of the output signal. The design of the power unit was also aimed to place all six independent voltage sources, for each measuring point, into one unit and ensure charging of all cells with full charge indication. Lithium cells with a capacity 2600 mAh and a maximum voltage 4 V are used as a voltage source. For these cells, a voltage drop is not expected during a series of measurements. The charging circuit of all cells is also integrated in the unit, with the possibility of disconnecting it as a potential source of electric noise as it is shown in the simplified circuit scheme in Figure 4. Noise reduction due to the use of battery power unit was up to 80%. The picture of the assembly is shown in Figure 5.

3.3. STRAIN GAUGES SIGNAL CORRECTION

After the power supply was implemented, the signal noise was significantly reduced. But the noise level was still significant and distorted the measured data. Another significant source of noise can be induced by wiring (lead wires, measuring cables, etc.). For this reason, shielded twisted pairs were used for cabling. Further reduction of the signal noise required

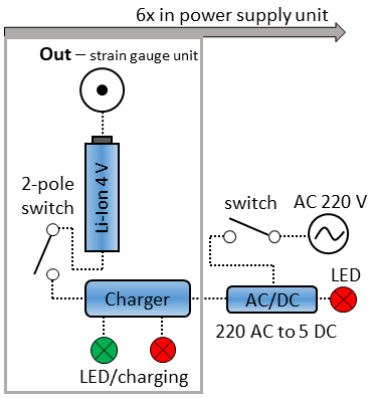

Figure 4. Battery power supply solution scheme.

Figure 5. Power supply unit - front side.

the passive element working as a frequency filter to be included. Relevant frequencies for the signal reconstruction are in the frequency range up to 200 kHz. Higher frequency filtering can be performed using a low pass filter realized by a capacitor of a suitable capacitance in the so-called double-wiring when the capacitor is connected in parallel to the series-connected resistor. The threshold frequency f_0 of the low pass filter realized by this connection is expressed by the relation:

$$f_0 = \frac{1}{2\pi RC}, \tag{1}$$

where R is the value of the series-connected resistance in our case the resistivity of the strain gauge used and C is the capacity of the capacitor. In case of using foil strain gauges with lowest resistivity 120 Ω compared to other types of strain gauges, a capacitor of 6.6 nF was used realizing a low pass filter f_0=201 kHz. For semiconductor strain gauges with resistivity 1000 Ω, the value f_0 is 241 kHz. The capacitor C is connected to the internal section of the BNC output terminal of the strain gauge unit. Comparison of the noise of the measured signal before and after the implementation of the frequency filter is in Figure 6.

3.4. Laser sensor and camera trigger unit

The data obtained from strain gauges provides information about the course of the deformation wave. However, it is not possible to estimate in detail the deformation behavior of the sample with a complex internal structure. Therefore, during the experiments, the deforming samples were observed using a digital

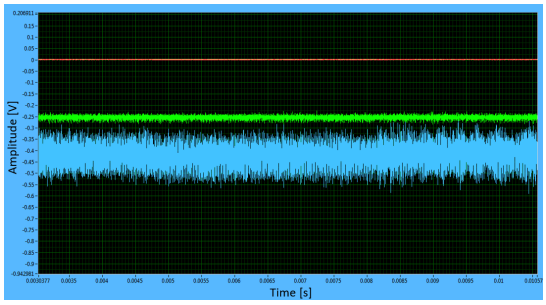

Figure 6. Noise reduction after low-pass filter implementation (green) and before (blue).

camera (FASTCAM SA5, Photron, Japan). Captured images were evaluated using a DIC technique to obtain in-plane displacement and strain fields [8]. The data were also used to estimate the expected measured values during the SHPB experiment. Synchronization is achieved using a signal from the optical gates as TTL (Transistor-Transistor Logic) pulse signal at the camera's up-link. The module further adjusts the magnitude of the output voltage of the optical gates before being brought to the high-speed digitizer where is it used as an experiment trigger and for the evaluation of impact velocity. The scheme of the module is shown in Figure 7.

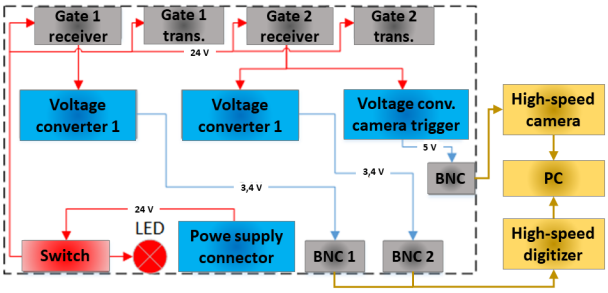

Figure 7. Block scheme of laser sensor and camera trigger unit.

3.5. LabView - GUI

The main reason for choosing the LabView environment is wide support of measurement devices from many manufacturers and their easy implementation [9]. In the case of the created solution for SHPB, LabView is used to control two four-channel digitization cards evaluating both optical gate signals and strain gauge sensors. The responsive user interface shown in Figure 8, is divided into functional partitions for better orientation. When saving an experiment record, a data header is added to the measured data, which contains the parameters of the measurement performed for subsequent evaluation in the Matlab environment (Mathworks Inc.). The resulting file is saved in the *.tdms format (Technical data management sharing).

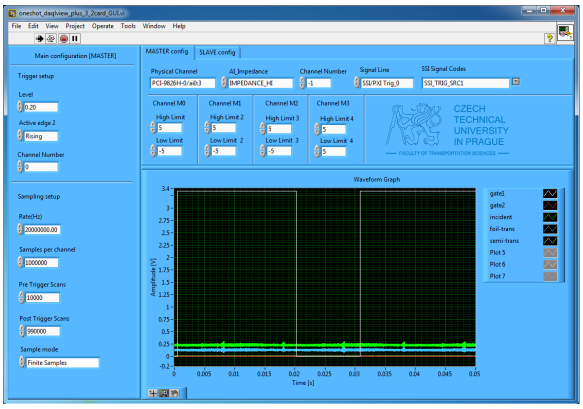

FIGURE 8. Graphical user interface in LabView.

4. EXPERIMENTAL VERIFICATION

Verification of correct function of all parts of the instrumentation as a whole was carried out by testing the deformation behavior of auxetic structures at different strain-rates. Auxetic structures are cellural materials with negative poisson's ratio [10]. Three types of auxetic structures were tested: 2D cut missing-rib, 2D inverted honeycomb and 3D inverted honeycomb. These structures were produced by Selective laser sintering method from a 315L-0407 austenitic stainless steel alloy. The visualization of individual structures is shown in Figure 9.

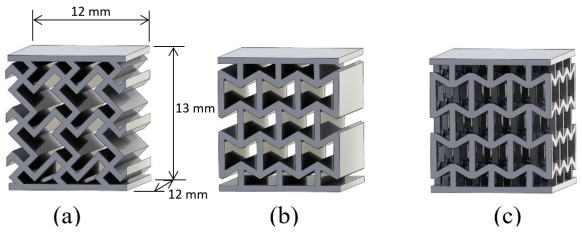

FIGURE 9. Tested auxetic structures, (a) 2D cut missing-rib, (b) 2D inverted honeycomb, (3) 3D inverted honeycomb.

A prepared samples were placed between the incident bar and the transmission bar and carefully aligned with the faces of the bars. Adjacent ends of the bars to the sample were marked by black and white texture for subsequent DIC analysis. Incident wave was generate by the striker bar with length 500 mm accelerated by gas-gun pressurized on 5 bars with resulting impact velocity of 33 ms^{-1}. High speed camera recording deformation process were set at 100 000 fps with 320x192 px image resolution. Two high intensity LED illuminators was used for sufficient illumination of the scene [11].

5. EXPERIMENTAL RESULTS

Laser sensor and camera trigger unit reliably recorded the transit of the striker through the first and second optical gate, synchronously triggering the high-speed camera record and signal from the strain gauges. The strain gauge signal has achieved sufficient quality for subsequent evaluation and the waveform at the realized measuring points on the incident and transmission bar was recorded. The measured signal from the strain gauges is shown in Figure 10.

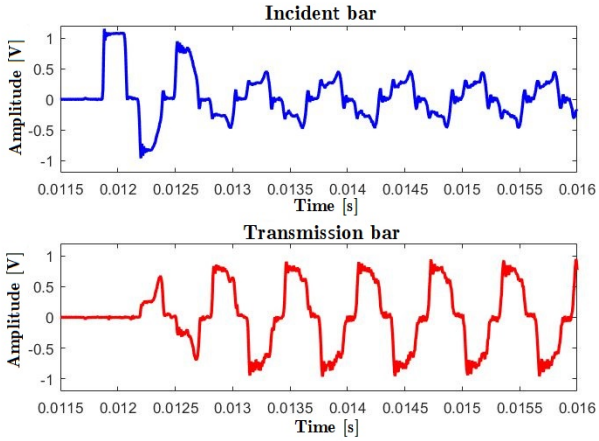

FIGURE 10. Measured signal from the incident and transmission bars.

The measured data were exported, along with the header containing the record parameters, to the *.tdms file for subsequent evaluation. Example of evaluated data showing stress-strain and strain rate-strain diagram for 2D Cut missing-rib structure is shown in Figure 11.

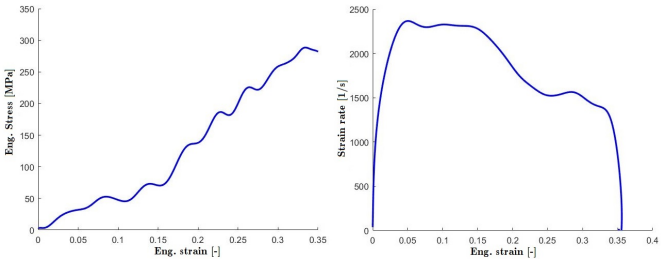

FIGURE 11. 2D cut missing-rib structure a) stress-strain diagram b) strain rate-strain diagram

By synchronizing the camera with optical gates a video recording of the entire deformation process was prepared. The high intensity LED illuminators ensure sufficient scene brightness for subsequent DIC evaluation. An example of selected images of a recorded deformation process of a 3D inverted honeycomb sample is shown in Figure 12.

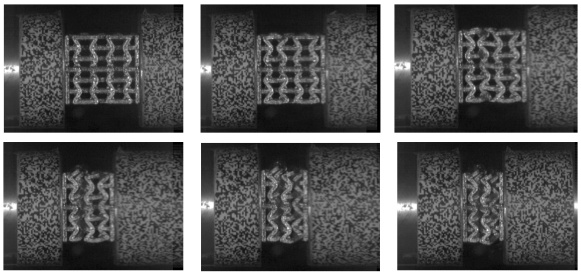

Figure 12. Deformation of the sample 3D inverted honeycomb.

6. Conclusions

In this paper, technical and software solutions for the SHPB assembly were designed and implemented for testing of soft material structure at high strain-rates. All partial solutions were continually tested to verify their proper functioning before they were used in the verification experiment. As part of a validation experiment, where different auxetic structures were tested, all instrument parts showed the required properties and the measured data were subsequently successfully evaluated. The experiment has also shown that the instrumentation has improved the quality and reliability of the acquired data, as well as the convenience of the operator of the SHPB instrumentation.

List of symbols

C Capacitance [F]

R Resistance [Ω]

f_o Threshold frequency [Hz]

Acknowledgements

The research was supported by the Czech Science Foundation (project no. 15-15480S) and the internal grant of the Czech Technical University in Prague (project no. SGS17/148/OHK2/2T/16 and SGS18/154/OHK2/2T/16). All the financial support is gratefully acknowledged.

References

[1] A. T. Owens. *Development of a Split Hopkinson Tension Bar for Testing Stress-Strain Response of Particulate Composites under High Rates of Loading.* M.sc. thesis, Faculty of Auburn University, 2007.

[2] K. Evans, A. Alderson. Auxetic materials: Functional materials and structures from lateral thinking! *Advanced Materials* **12**(9):617–628, 2000. Cited By 406, doi:10.1002/(SICI)1521-4095(200005)12:9<617::AID-ADMA617>3.0.CO;2-3.

[3] P. Wang, S. Xu, Z. Li, et al. Experimental investigation on the strain-rate effect and inertia effect of closed-cell aluminum foam subjected to dynamic loading. *Materials Science and Engineering A* **620**:253–261, 2014. Cited By 36, doi:10.1016/j.msea.2014.10.026.

[4] O. Duncan, L. Foster, T. Senior, et al. Quasi-static characterisation and impact testing of auxetic foam for sports safety applications. *Smart Materials and Structures* **25**(5), 2016. Cited By 9, doi:10.1088/0964-1726/25/5/054014.

[5] B. Yang, L. Tang, Y. Liu, et al. Localized deformation in aluminium foam during middle speed hopkinson bar impact tests. *Materials Science and Engineering A* **560**:734–743, 2013. Cited By 18, doi:10.1016/j.msea.2012.10.027.

[6] B. Hou, H. Zhao, S. Pattofatto, et al. Inertia effects on the progressive crushing of aluminium honeycombs under impact loading. *International Journal of Solids and Structures* **49**(19-20):2754–2762, 2012. Cited By 44, doi:10.1016/j.ijsolstr.2012.05.005.

[7] G. Ma, Z. Ye, Z. Shao. Modeling loading rate effect on crushing stress of metallic cellular materials. *International Journal of Impact Engineering* **36**(6):775–782, 2009. Cited By 60, doi:10.1016/j.ijimpeng.2008.11.013.

[8] S.-W. Khoo, S. Karuppanan, C.-S. Tan. A review of surface deformation and strain measurement using two-dimensional digital image correlation. *Metrology and Measurement Systems* **23**(3):461–480, 2016. Cited By 9, doi:10.1515/mms-2016-0028.

[9] C. Elliott, V. Vijayakumar, W. Zink, R. Hansen. National instruments labview: A programming environment for laboratory automation and measurement. *Journal of Laboratory Automation* **12**(1):17–24, 2007. Cited By 124, doi:10.1016/j.jala.2006.07.012.

[10] H. Wan, H. Ohtaki, S. Kotosaka, G. Hu. A study of negative poisson's ratios in auxetic honeycombs based on a large deflection model. *European Journal of Mechanics, A/Solids* **23**(1):95–106, 2004. Cited By 71, doi:10.1016/j.euromechsol.2003.10.006.

[11] T. Fíla, P. Zlámal, O. Jiroušek, et al. Impact testing of polymer-filled auxetics using split hopkinson pressure bar. *Advanced Engineering Materials* **19**(10), 2017. Cited By 2, doi:10.1002/adem.201700076.